

THE LEAKY SURFACE WAVE IN $\text{SiO}_2/\text{49}^\circ\text{Y-X LiNbO}_3$ STRUCTURE*

Z.L. JIANG, W.Q. WU, Y.A. SHUI and J.H. YIN

Institute of Acoustics, Nanjing University,
Nanjing 210008, P.R. China

ABSTRACT

In this paper the velocity, attenuation and dispersion curve of LSW, the electro-mechanical coupling coefficient K_2 versus film thickness normalized to wave length (kh) and TCD versus kh , TCD versus temperature T for $\text{SiO}_2/\text{49}^\circ\text{Y-X LiNbO}_3$ structure with different boundary conditions have been calculated. These results show that within the range $0.6kh < 0.5$ the attenuation of LSW is very small, near to 0. Under different boundary conditions, SiO_2 of suitable film thickness ($kh=1.53, 1.37, 2.0$) can all get zero TCD, whereas K_2 versus kh will be different. When JHY are in the interface, K_2 will increase as kh increases and has a maximum. The maximum K_2 is 15% i.e., about 1.08 times as large as K_{20} which is the electro-mechanical coupling coefficient of zero film thickness.

INTRODUCTION

Since the SAW devices come into exist, they have been developed quickly and used widely in both military and consumer electronic equipment, such as RADAR, communication, and TV set due to their strong signal processing functions. In process of their development, people are more and more interested in the characteristics of SAW materials because the performance of SAW devices are greatly related to them. Usually the following characteristics are desired: 1) large electro-mechanical coupling coefficient, which will lead to lower loss. 2) small temperature coefficient of delay which will lead to better temperature stability. 3) fast propagation velocity, so one can get higher frequency devices within existing photolithograph resolution. In order to seek materials with these characteristics, a lot of efforts have been made. A relatively successful one is to search for new propagation modes. It has been found that electro-mechanical coupling coefficient K_2 of some leaky wave modes can be as large as 17-18%, which is much higher than 5.8% of

the Rayleigh mode in $128^\circ\text{Y-X LiNbO}_3$. For example people have found such leaky modes in Y-cut LiNbO_3 [1], $\text{Y-41}^\circ\text{LiNbO}_3$ [2] and $49^\circ\text{Y-X LiNbO}_3$. The last one has the highest K_2 and the lowest attenuation.

Since the $49^\circ\text{Y-X LiNbO}_3$ has a high temperature coefficient of delay (TCD), about 85 ppm, its application is limited. To overcome this shortcomings, we deposit a SiO_2 film on $49^\circ\text{Y-X LiNbO}_3$ to compensate its TCD. Previously, T.E. Parker et al. [3,4] improved TCD of Y-Z LiTaO_3 and Y-Z LiNbO_3 by using $\text{SiO}_2/\text{Y-Z LiTaO}_3$ and $\text{SiO}_2/\text{Y-Z LiNbO}_3$ structures. In their papers, excellent temperature coefficients for these structures are reported. But rather large film thickness (about $kh=3$) is needed and propagation loss is large. K. Yamamoto et al. also have studied $\text{Si}/\text{O}_6^\circ\text{Y-X LiTaO}_3$, $\text{SiO}_2/\text{126}^\circ\text{Y-X LiTaO}_3$, $\text{SiO}_2/\text{121}^\circ\text{Y-X LiNbO}_3$ structures [5,6], and have obtained similar results. Recently, K. Yamamoto and J.H. Yin [7] have presented the propagation characteristics of $\text{SiO}_2/\text{128}^\circ\text{Y-X LiNbO}_3$ structure respectively. They got better results.

In this paper, we have calculated the leaky wave characteristics and TCD of $\text{SiO}_2/\text{49}^\circ\text{Y-X LiNbO}_3$ structure.

THEORETICAL CALCULATION

The geometry for leaky wave propagation in layered structure and coordinate system are shown in fig1, where h is the thickness of film, x is the propagation direction, z is the normal direction to interface. From the leaky wave definition, the partial wave of leaky wave can be expressed as:

$$\begin{aligned} U &= A_j \exp[ikx \exp[ik(l+is)x \exp[-i\omega t \\ C &= A_k \exp[ikx \exp[ik(l+is)x \exp[-i\omega t \\ &\quad \text{for } l, 2, 3 \end{aligned}$$

Where, R is the propagation attenuation, A_j is the amplitude of the wave, ϕ is electric potential. Using Christoff equation and two-dimension Powell method, we calculated velocity V and attenuation R under different boundary conditions. Fig2-Fig7 present the dispersion curves of leaky wave in $\text{SiO}_2/\text{49}^\circ\text{Y-X LiNbO}_3$ structure under various boundary conditions.

Fig2 and fig3 is for shorted interface, fig4 and fig5 is for the situation of interface opened,

*This work is supported by the National Natural Science Fund.

surface shorted, fig6 and fig7 is the situation of both interface and surface opened. Since SiO₂ is nonpiezoelectric film, with interface shorted, we get some results whether surface is opened or shorted. From these figs, we can find that the leaky wave velocities and attenuation decrease with increase of kh. When kh=2, leaky mode will transfer to Rayleigh mode, attenuation becomes zero. When interface is opened, we find a dip of attenuation in the range 0.4<kh<0.4.

Leaky wave is coupled with surface waves and bulk wave. With depth increases, surface wave reduce and bulk wave increase. So on the surface, leaky wave is smaller to surface wave. Here, shear wave velocity in substrate V_t is 4085 m/s, in film V_f is 3758 m/s, and V_f/V_t , which is corresponding to the 'load' situation. In this situation, velocities decline with thickness increase. We also find that the film can suppress bulk wave, make attenuation smaller. In fig4, the boundary condition is that interface is opened and surface shorted. There are two effects in this case. One is surface 'short' effect, another is 'load' effect. When kh is very small, the surface short effect is the predominate one, so velocity increases. When kh=0.35, two effects is equally strong. When kh>0.35, the 'load' effect is the main one, so velocity declines. In all cases, velocities change from 4800 m/s to 4100 m/s, attenuations change from 0.00054dB/l to zero. These characteristics is very useful in practical applications.

The electro-mechanical coupling coefficient can be calculated from fig2 to fig7, and are shown in fig8, where K_{20} is the electro-mechanical coupling coefficient of leaky wave for 49 Y-X LiNbO₃ substrate, K_2 is that of leaky wave of SiO₂/49° Y-X LiNbO₃ structure. Curve I, II, III represent the following different situations: I) transducers are on the surface of SiO₂ and interface is opened. II) transducers are in the interface and surface is shorted. III) transducers are in the interface and surface is opened. In case I, electro-mechanical coupling coefficient K_2 will decrease and go to zero quickly when film thickness kh increases. When transducers are in the interface between SiO₂ and 49° Y-X LiNbO₃, K_2 will increase as kh increases and has maximum. As kh is in range of 0.4 to 0.8, the maximum is 1.08 times as large as K_{20} and is about 15%. This maximum is also two times as large as that of 49° Y-X LiNbO₃ which is the most widely used material for the SAW devices.

Considering the temperature dependence of elastic, piezoelectric, dielectric constant [8,9], we can get dispersion relations at different temperature by duplicating above calculations. The temperature dependence of $\Delta V/V$ (or temperature coefficient of delay) also can be obtained at different temperature and film thickness kh. The relationship between temperature coefficient of delay and film thickness has been given in fig9. The boundary conditions of fig10 and fig11 are the same as fig2, fig4 and fig6. Calculations are carried out at 25°C.

It can be seen that TCD changes from positive to negative as kh increases. In fig9, TCD=4 ppm at kh=2, in fig10, TCD=0 at kh=1.37, in fig11 TCD=0 at kh=1.53. These results show that zero TCD can be obtained with thinner film thickness in this structure. It means that thinner film is needed to compensate TCD for a specified frequency or with a specified film thickness we can get higher operating frequency at zero TCD point, while the electro-mechanical coupling coefficient is very large.

Fig12 gives TCD versus temperature as kh=2. Here, the boundary condition is interface shorted. When temperature changes from -40°C to 40°C, TCD increases. This is different from SiO₂/128° Y-X LiNbO₃ structure, TCD of which decreases with temperature increase. The range of TCD is 0.5 ppm to 4 ppm for SiO₂/49° Y-X LiNbO₃ structure. It is smaller than that of SiO₂/128° Y-X LiNbO₃ structure. This means that better temperature stability can be obtained.

CONCLUSION

In this paper we studied the leaky surface wave characteristics in SiO₂/49° Y-X LiNbO₃ structure. It is found that leaky mode still exists when deposited SiO₂ film in the range of kh<2. The attenuations are smaller than that of kh=0. In the range 0.4<kh<0.4, there is a zero point of attenuation. When transducers are in the interface, the electro-mechanical coupling coefficient increases to 1.08 times as large as that of kh=0. We have also found there exist several zero TCD points for SiO₂/49° Y-X LiNbO₃ structure. In the range -40°C to 40°C, TCD changes less than 4 ppm. So better temperature stability can be expected. The thickness of film to obtain the zero TCD point is thin, less than one third of a wavelength. Hence, this structure is very useful in making high frequency, wide band, low loss and low temperature stable SAW devices. To verify the theoretical results, the experiments are needed.

REFERENCES

1. K.YAMAMOTO and SHIBAYAMA, J.Appl.Phys., Vol.43, No.3, 1972, P856
2. P.D.BLACK, et al, Proc. IEEE Ultrasonics Symposium, 1981, P2.8
3. T.E.PARKER, Appl. Phys. Lett., Vol.20, No.3, Feb. 1975, P75
4. T.E.PARKER, J.Appl.Phys., Vol.50, No.3, March 1979, P1360
5. K.YAMAMOTO, IEEE Trans. on Sonic and Ultrasonic, Vol. SU-25, No.1, (1978), P384
6. K.YAMAMOTO, Wave Electron, Vol.3, 1979, P819
7. J.H.YIN, et al, Proc. IEEE Ultrasonics Symposium, 1987, P237
8. F.T.SMITH, J.Appl.Phys., Vol.42, No.6, May 1971, P2219
9. A.J.SLOBODIN, AD-742 267

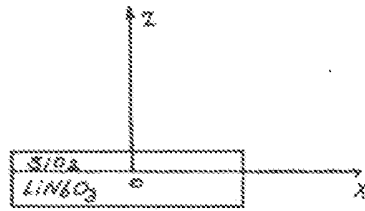


Fig 1

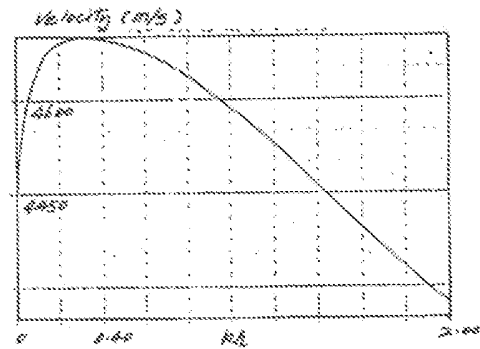


Fig 4

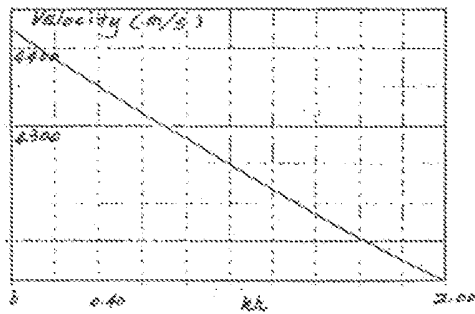


Fig 2

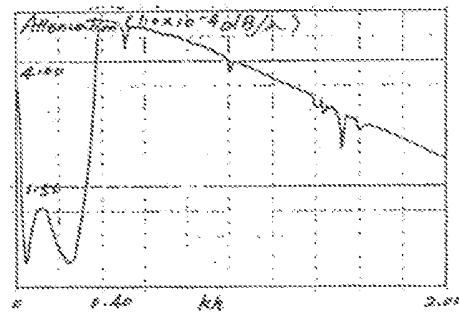


Fig 5

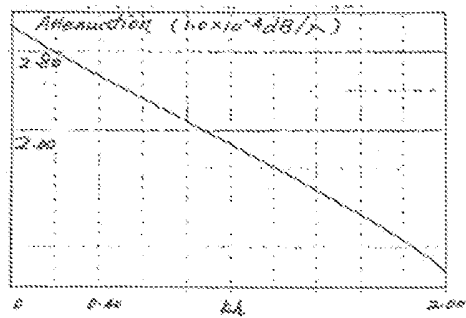


Fig 3

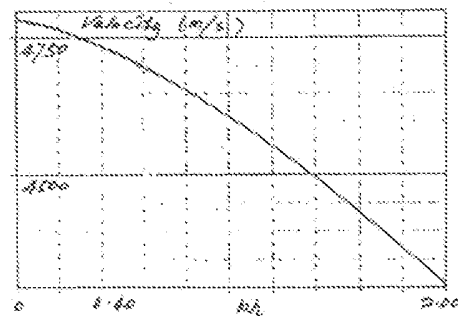


Fig 6

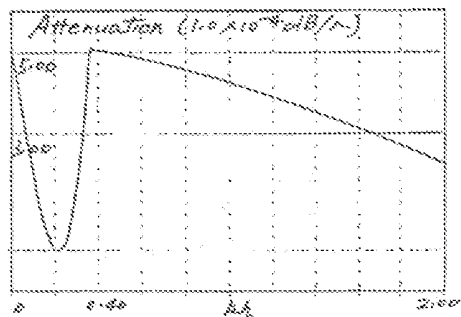


Fig 7

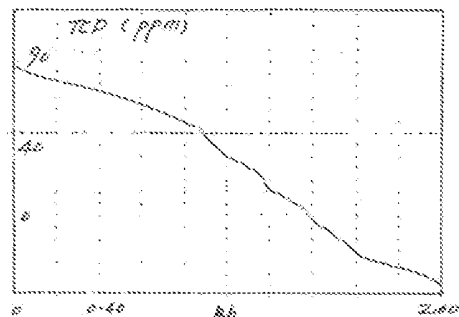


Fig 10

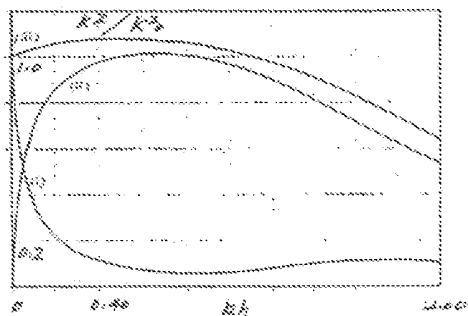


Fig 8

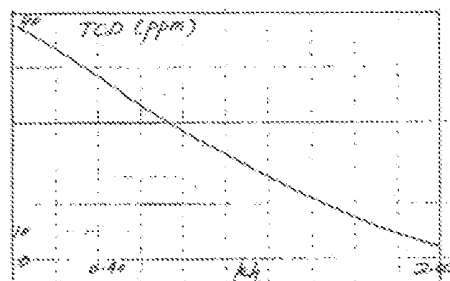


Fig 9

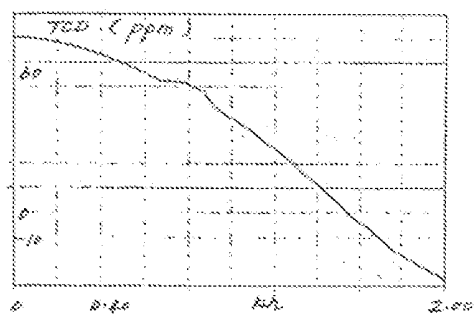


Fig 11

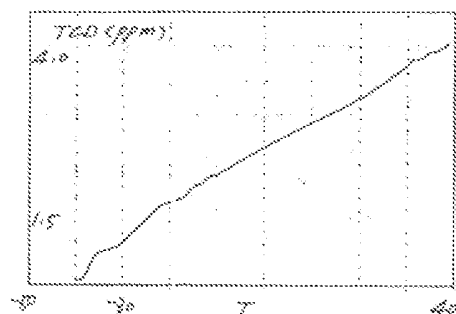


Fig 12